Durham University

Durham Research Online

Deposited in DRO:

06 July 2017

Version of attached file:

Accepted Version

Peer-review status of attached file:

Peer-reviewed

Citation for published item:

Li, Chensen and Nobuyasu, Roberto S. and Wang, Yukun and Dias, Fernando B. and Ren, Zhongjie and Bryce, Martin R. and Yan, Shouke (2017) 'Solution-processable thermally activated delayed fluorescence white OLEDs based on dual-emission polymers with tunable emission colors and aggregation enhanced emission properties.', Advanced optical materials., 5 (20). p. 1700435.

Further information on publisher's website:

https://doi.org/10.1002/adom.201700435

Publisher's copyright statement:

This is the peer reviewed version of the following article: C. Li, R. S. Nobuyasu, Y. Wang, F. B. Dias, Z. Ren, M. R. Bryce, S. Yan (2017) Solution-Processable Thermally Activated Delayed Fluorescence White OLEDs Based on Dual-Emission Polymers with Tunable Emission Colors and Aggregation-Enhanced Emission Properties, Advanced Optical Materials, 5(20): 1700435, which has been published in final form at https://doi.org/10.1002/adom.201700435. This article may be used for non-commercial purposes in accordance With Wiley-VCH Terms and Conditions for self-archiving.

Additional information:

Use policy

The full-text may be used and/or reproduced, and given to third parties in any format or medium, without prior permission or charge, for personal research or study, educational, or not-for-profit purposes provided that:

- a full bibliographic reference is made to the original source
- a link is made to the metadata record in DRO
- the full-text is not changed in any way

The full-text must not be sold in any format or medium without the formal permission of the copyright holders.

Please consult the full DRO policy for further details.

Durham University Library, Stockton Road, Durham DH1 3LY, United Kingdom
Tel : +44 (0)191 334 3042 | Fax : +44 (0)191 334 2971
https://dro.dur.ac.uk

DOI: 10.1002/ ((please add manuscript number))
Article type: Full Paper

Solution-Processable Thermally Activated Delayed Fluorescence White OLEDs Based on Dual-Emission Polymers with Tunable Emission Colors and Aggregation Enhanced Emission Properties

Chensen Li, Roberto S. Nobuyasu, Yukun Wang, Fernando B. Dias, Zhongjie Ren, Martin R. Bryce* and Shouke Yan**

Dr. C. Li, Dr. Z. Ren, Prof. S. Yan
Beijing Advanced Innovation Center for Soft Matter Science and Engineering, State Key Laboratory of Chemical Resource Engineering, Beijing University of Chemical Technology, Beijing 100029, China.
E-mail: renzj@mail.buct.edu.cn, skyan@mail.buct.edu.cn
R. S. Nobuyasu, Dr. F. B. Dias
Department of Physics, Durham University, South Road, Durham, DH1 3LE, U.K.
Dr. Y. Wang
State Key Laboratory of Polymer Physics and Chemistry, Changchun Institute of Applied Chemistry, University of Chinese Academy of Sciences, Changchun, 130022, China
Prof. M. R. Bryce
Department of Chemistry, Durham University, South Road, Durham, DH1 3LE, U.K.
E-mail: m.r.bryce@durham.ac.uk

Keywords: thermally activated delayed fluorescence, aggregation enhanced emission, solution-processable organic light-emitting diodes, two-color white copolymer

Thermally activated delayed fluorescence (TADF) white organic light-emitting diodes (WOLEDs) have drawn tremendous interest and have been extensively studied because of harvesting both triplet and singlet excitons without heavy metals. However, single white-light-emitting polymers are currently limited and few strategies exist to design these materials. Herein, we have proposed a new strategy to develop the polymers with tunable emission colors combined fluorescence and TADF based on aggregation enhanced emission (AEE) characteristics. The polymers containing different ratios of pendant 2-(10H-phenothiazin-10-yl)dibenzothiophene-S,S-dioxide units with yellow TADF emission and dibenzothiophene (DBT) units with blue fluorophor emission, which display both TADF and AEE characteristics, were synthesized successfully. Among them, the emission color of P3 in different THF/water mixtures changes from greenish-blue to white or yellow. Moreover, P3 displays white emission in the solid state dispersing by poly(methyl methacrylate). In addition,

electroluminescent device of P3 can achieve white light emission with high color rending indexes (CRI) and low turn-on voltages (V_{on}) as well. P3 OLEDs show two-color warm-white emission with high CRI of 77, low V_{on} of 2.9 V, CE_{max} of 23.0 cd/A, PE_{max} of 32.8 lm/W, EQE_{max} of 10.4% with CIE coordinates of (0.37, 0.38) at 5 V. Moreover, EQE of 2.6%, CE of 5.7 cd/A, PE of 4.7 lm/W at 100 cd/m^2 are obtained. To the best of our knowledge, our work reports the first example of warm-white TADF polymer OLEDs.

1. Introduction

Organic light-emitting diode (OLED) devices, especially, white OLEDs (WOLEDs) are attracting great interest in display and lighting applications.[1-3] Most white luminescent materials are blends of several small molecules that emit different colors spanning the entire visible spectrum.[4-7] These devices often are unstable due to significant phase segregation. In comparison, white luminescent polymers possess the advantages of enhanced control of emitter ratios, low-cost, and solution-processability for large-area flexible displays.[4-8] Fluorescent and phosphorescent WOLEDs have been extensively reported based on white-emitting polymers.[9,10] However, the internal quantum efficiency (IQE) of fluorescent OLEDs is only 25%.[11] Although phosphorescent OLEDs can achieve almost 100% IQE, the expensive and scarce metals used in these devices, such as iridium or platinum, create additional economic and environmental problems that restrict the application of WOLEDs in large-scale applications, such as lighting. Moreover, there is also significant degradation of emitters in the blue spectral region.[12,13]

Thermally activated delayed fluorescence (TADF) emitters, as a route for the next generation OLEDs, harvest light from both triplet and singlet excitons without noble metals.[14-17] Recently, all-TADF WOLEDs and WOLEDs hybridizing TADF emitters with triplet emitters have been reported.[18-23] Adachi's group demonstrated WOLEDs using red, green, and blue TADF molecules as emissive dopants, with external quantum efficiency

(EQE) of >17% with Commission Internationale de l'Eclairage (CIE) coordinates of (0.30, 0.38).[18] Hybrid WOLEDs combining fluorescent emitters and TADF emitters are desirable to improve the EQE due to their excellent stability and harvesting of both singlet and triplet excitons. Lee's group developed hybrid WOLEDs with an external quantum efficiency >20% using blue or green small molecule TADF materials.[19,20] However, all the previous TADF emitters for WOLEDs are small molecules and no TADF polymer WOLEDs have been reported to date. In general, the small molecules are limited in such properties as thermal stability, mechanical robustness, and flexibility.

Polymers, in contrast, can have both good thermal stability, solution processable and facile functionality to introduction of various functional units into pendant groups.[24,25] Nowadays, Polymeric materials have been proven to be ideal emissive materials for the solution-processed devices.[26-30] Therefore, some groups reported luminous polymers containing pendant TADF units, which demonstrated good performance in the solution-processed OLEDs. Yang et al.[28] synthesized copolymers from three monomer components, with a backbone of polycarbazole and 10-(4-(5-phenyl-1,3,4-oxadiazol-2-yl)-phenyl)-10H-phenoxazine as pendant TADF units. Those bluish-green OLEDs had EQE_{max} of 4.3% and EQE 2.4% at100 cd/m^2. Zhu et al.[29] reported a TADF polymer PAPTC with triazine acceptor and 9,10-dihydroacridine donor as backbone and pendant units, respectively. PAPTC had M_n 22.0 kDa and PDI 2.96. A green OLED with EQE_{max} of 12.6% at 180 cd/m^2 was obtained. Our group[30] reported a series of polymers with an insulating backbone and varying ratios of 2-(10H-phenothiazin-10-yl)dibenzothiophene-S,S-dioxide as a pendant TADF unit. Green-emitting devices with one of our polymers achieved EQE_{max} as high as 20.1%, with EQE 5.3% at 100 cd m^{-2}. However, no white-light-emitting TADF polymers have been reported to date because controlling energy transfer process and tuning emission colors are still challenging.

Emitters with delayed fluorescence often encounter severe aggregation-caused quenching (ACQ) because of the strong intermolecular interactions, which is a hindrance to improving the efficiency of OLEDs for practical applications.[31-34] In contrast, aggregation-induced emission (AIE) is a property of some molecules that have almost no fluorescence in solution, but are highly emissive in the aggregate state.[35-37] Several studies on small TADF molecules have reported noticeable emission enhancement in aggregates or in the solid-state.[38,39] Emissive materials with tunable luminescent colors are of great significance for their optical applications. Tang et al.[40,41] found impressive color-tunable aggregation induced emission (AIE) and aggregation enhanced emission (AEE) behaviors in the solid state. Taking these into account, employing AIE or AEE to tune emission colors aiming to obtain white emission is realistic. Therefore, the development of solution-processed single white-emitting polymers with both TADF and AEE features is of importance.

We have now synthesized the non-conjugated TADF copolymers with pendant 2-(10*H*-phenothiazin-10-yl)dibenzothiophene-*S*,*S*-dioxide (PTZ-DBTO2) and dibenzothiophene (DBT) units as shown in **Scheme 1**. PTZ-DBTO2[34,38,39] was chosen because it exhibits strong TADF and AIE features. Dibenzothiophene (DBT) with high triplet energy of 3.04 eV and good hole-transporting ability[38,42] was introduced as a blue fluorescence emitter[43-44] and as a TADF host.[45,46] We reasoned that the blue emitting DBT units together with yellow emitting PTZ-DBTO2 units could lead to a white light emitting copolymer, while the DBT units disperse the PTZ-DBTO2 components and thus regulate the aggregation and quenching. The obtained copolymers P1-P3 display obvious TADF and AIE features and most significantly P3 shows warm-white electroluminescence.

2. Results and discussion

2.1. Synthesis and characterizations

The polymers P1-P3 were prepared by radical copolymerization of 2-vinyldibenzothiophene and 2(10*H*-phenothiazin-10-yl)-8-vinyldibenzothiophene-*S*,*S*-dioxide

with the molar feed ratios of 50 : 50, 71 : 29 and 90 : 10, respectively. The actual content of TADF unit, PTZ-DBTO2, in the copolymers estimated from elemental analysis data is ca. 71%, 46% and 18% for P1-P3, respectively, indicating the slightly greater reactivity of the PTZ-DBTO2 monomers. The copolymers are readily soluble in chloroform, toluene and tetrahydrofuran. The weight average molecular weights (M_w) of P1-P3 were determined to be 11.6, 30.1, and 22.8 kDa with PDIs of 1.33, 1.67, and 1.65, respectively (**Table 1** and **Figure S2**). The structures of the polymers were confirmed by ^{1}H NMR spectra (**Figure S1**).

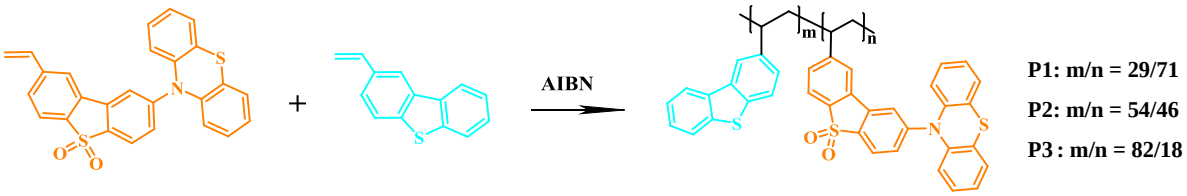

Scheme 1. Synthetic route for P1-3.

Table 1. Data for P1, P2 and P3.

	M_w/PDI[a]	T_g[b] (°C)	T_d[c] (°C)	λ_{abs}[d] (nm)	λ_{PL}[d] (nm)	E_g[e] (eV)	HOMO[f] (eV)	LUMO[g] (eV)	E_T[h] (eV)	ΔE_{ST}[i] (eV)	$\Phi_{PL,film}$[j] (%)	$\Phi_{PL,tol}$[j] (%)	$\Phi_{PL,tol}$[k] (%)
P1	11,600/1.33	226	381	290,330	547	2.76	-5.08	-2.32	2.54	0.09	10.4	9.9	19.8
P2	30,100/1.67	223	381	289,330	542	2.77	-5.10	-2.33	2.57	0.06	23.5	16.1	28.3
P3	22,800/1.65	206	357	230,229	535	2.82	-5.08	-2.26	2.60	0.04	19.5	15.9	52.9

[a]Determined by GPC, eluting with THF, by comparison with polystyrene standards. [b]The value of T_g was determined at a heating rate of 10 °C/min under a nitrogen atmosphere. [c]Temperature at which a 5% weight loss occurred was determined at a heating rate of 10 °C/min under a nitrogen atmosphere. [d]Measured in films at room temperature. [e]Optical energy gap (E_g) deduced from the absorption onset of a neat film. [f]Calculated according to the equation $E_{HOMO} = -(E_{(onset,\ ox\ vs\ Fc^+/Fc)} + 5.1)$ by CV. [g]Calculated according to the equation LUMO=HOMO + E_g. [h]Triplet energy was calculated from the onset wavelength of phosphorescent emission. [i]$\Delta E_{ST} = S_1 - T_1$. [j]Absolute PL quantum yield in the film state and in toluene solution determined by a calibrated integrating sphere in air; error ± 0.5%. [k]Absolute PL quantum yield in toluene solution determined by a calibrated integrating sphere in nitrogen; error ±0.5%.

2.2. Synthesis and characterizations

The thermal properties of the polymers were investigated by differential scanning calorimetry (DSC) and thermogravimetric analysis (TGA). As shown **Table 1** and **Figure S3**, the decomposition temperatures (T_d) with 5% weight loss under nitrogen are in the range 381-

357 ℃, showing their excellent thermal stability. A trend is clear that T_d decreases slightly with an increased ratio of DBT units. **Figure 1a** and **Table 1** show that a distinct glass transition temperature (T_g) is observed for each polymer with values ranging from 226 °C to 206 °C. In addition, there are no exothermic peaks resulting from crystallization during the scan ranges for all the polymers, indicating an amorphous state of the polymers. The high T_d and T_g values favour long-term stability for practical applications.

The electrochemical behavior of the three polymers was investigated by cyclic voltammetry (CV) in degassed anhydrous acetonitrile solution. The data show quasi-reversible oxidation and reduction processes for all polymers (**Figure 1b**) corresponding to electrochemical doping and dedoping during the potential sweeps. P1 has similar oxidation and reduction potentials to unsubstituted phenothiazine donor and dibenzothiophene-S,S-dioxide acceptor units, respectively. All the polymers display roughly similar oxidation and reduction behavior as the process is centered on the PTZ-DBTO2 TADF units. A slight decrease in oxidation potential is observed when DBT is added, i.e., the copolymers are easier to oxidize than PTZ-DBTO2. Meanwhile, the copolymers are also easier to reduce than PTZ-DBTO2.

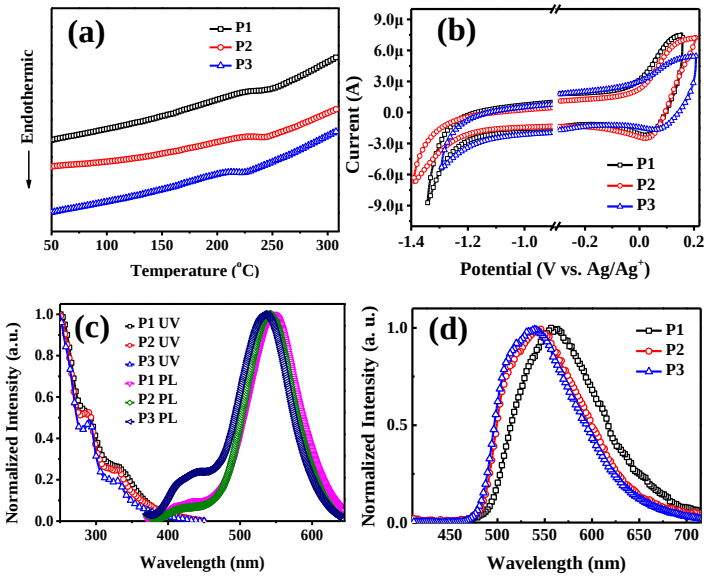

Figure 1. (a) DSC measurement of P1-3 recorded at a heating rate of 10 °C min^{-1}. (b) Cyclic voltammograms of P1-3 in acetonitrile. (c) UV-Vis absorption and PL spectra of P1-3 in solid state at 20 °C. (d) Phosphorescent spectra of P1-3 in solid state at 80K.

2.3. Photophysical properties

Figure 1c shows the UV-Vis absorption and photoluminescence (PL) spectra of P1-3. The absorption spectra in neat films show π-π* transitions of the DBT moiety at 290 nm and electronic transitions of PTZ-DBTO2 at 330 nm. In addition, relatively wide energy gaps (E_g) of 2.76, 2.77 and 2.82 eV for P1, P2 and P3, respectively, were obtained from the onset of absorption. The PL spectra of P1-P3 in thin films display a similar profile with λ_{max} at 547, 542 and 535 nm, respectively. The PL peaks gradually red-shift with increasing ratio of PTZ-DBTO2 units, indicating that the DBT units can effectively disperse the TADF units. The emission of P3 shows a more obvious signature of DBT units between 412 to 435 nm, as expected.

To estimate the TADF characteristic of copolymers, the triplet energies of the three polymers were determined according to the phosphorescent spectra as shown in **Figure 1d**. As shown in **Table 1**, E_T of P1-3 are 2.54, 2.57 and 2.60 eV, respectively, and E_T decreases with decreasing the content of DBT. In P3, with the larger proportion of DBT spacers, the TADF units behave more as isolated chromophores, and the phosphorescence is at higher energy. Since the energy of the singlet state is not so affected, the singlet-triplet energy gap is smaller in P3 than in the other polymers, which facilitates reverse intersystem crossing (RISC) and leads to a higher TADF contribution in P3. The ΔE_{ST} values for P1-3 are calculated to be 0.09, 0.06, and 0.04 eV, respectively. It is well known that a small ΔE_{ST} is necessary for efficient RISC which is required for TADF, and the smaller the value of ΔE_{ST}, the higher the rate of RISC. Therefore, possibly, P3 is a better TADF polymer that the others.

The time-dependent fluorescence decays of thin films of P1-3 at room temperature are seen in **Figure 2a**. Prompt (PF) and delayed fluorescence (DF) components are clearly

observed, with DF intensity increasing gradually in the sequence P1<P2<P3. **Figure 2b** shows the integral of DF in P3, collected with 0.1 μs delay time, and integrated over 50 μs, as a function of excitation power. A clear linear dependence with slope 1 is obtained, confirming that the DF originates from a monomolecular process rather than from triplet-triplet annihilation (for which the slope is 2).[47] **Figure 2c** depicts the temperature dependence of fluorescence decay of a thin film of P3. The PF shows almost no variation with temperature, which is consistent with negligible internal conversion. However, the DF component shows clear temperature dependence, decreasing in intensity and increasing in lifetime at low temperatures. All these observations are consistent with the TADF mechanism. The PL spectra of P3 in dilute polar solvents (THF, DMF, acetonitrile) are red shifted compared to nonpolar solvents such as toluene and cyclohexane, indicating the intramolecular charge transfer character of the emissive singlet state (**Figure 2d**). Also, as predicted, the photoluminescence quantum yields (Φ_{PL}) of P3 in polar solvents show a lower value due to the character of the excited state that in polar solvents leads to a more distorted structure and poor spacial overlap of the orbitals involved in the electronic transition **(Table S1)**. In addition, the peak width at half-height of the red-shifted emission decreased, suggesting that increased polarity can reduce aggregation and improve the color purity. Moreover, the emission color of P3 exhibits white emission in toluene due to the balance of AEE and ACQ, which is consistent with AEE properties discussed below. P1 and P2 show similar behavior (**Figures S4&5**).

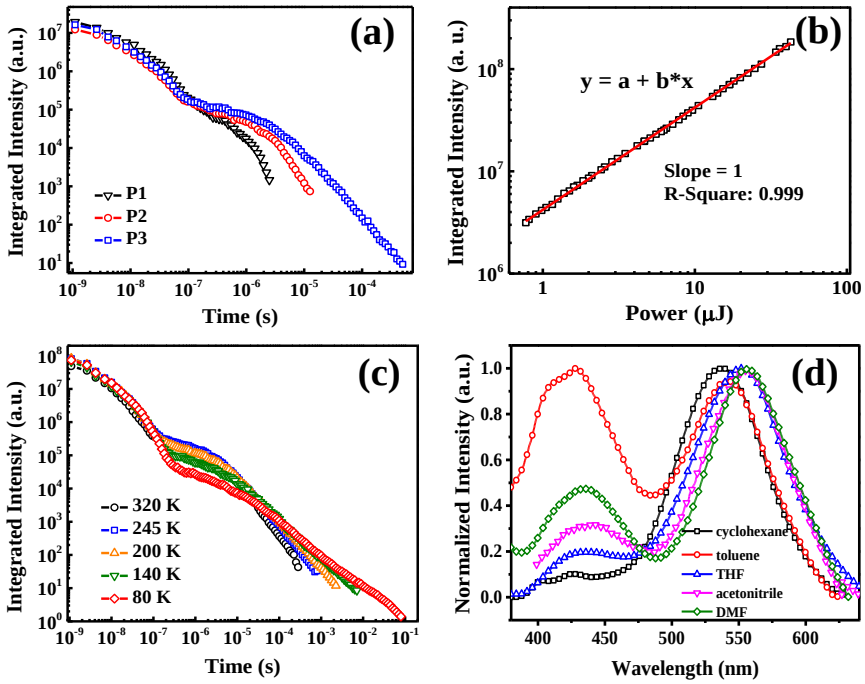

Figure 2. (a) Fluorescence decay data for P1-P3 in pristine thin films at 20 ^{o}C; no luminescence is observed for P1 and P2 at longer times. (b) Power dependence of DF with excitation power for P3. (c) Temperature dependence of fluorescence decays for P3. (d) Photoluminescence spectra of P3 in cyclohexane, toluene, THF, acetonitrile and DMF with 0.1 mg/ml.

2.4. Aggregation enhanced emission (AEE) properties

The Φ_{PL} values of P1, P2 and P3 in solid films are 10.4%, 23.5% and 19.5%, respectively. The Φ_{PL} values (**Table 1**) in dilute toluene solutions are 9.9%, 16.1% and 15.9%, respectively, indicating that these polymers are AEE-active. After N_2 bubbling, the values increase to 19.8%, 28.3% and 52.9%, respectively, which shows that triplet excitons are substantially quenched by oxygen.[14] To further study the aggregation enhanced optical properties, solvent-nonsolvent PL measurements were performed. The very weak emission of P3 in pure THF solution increases steadily with increasing the content of water and the peak at ca. 550 nm is sharply enhanced at 10:90 (v/v) THF/water mixture, confirming the AEE property of polymers (**Figure 3a&b**). The enhancement of PL intensity may be caused by the

aggregation of the PTZ-DBTO2 units of P3. The twisted conformation of PTZ-DBTO2 units[38] will favour loose packing with weak molecular interactions, and thus rotation and vibration will occur easily in the dilute solution. In contrast, in the aggregated state, intramolecular motions are restricted, and thus the non-radiative pathways of the excited state are blocked.[39] Therefore, as shown in **Figure 3b**, with the increase of water fraction, the emission of P3 is enhanced. Interestingly, the emission color of P3 can be tuned by adding water because of its dual emission, namely sky-blue from the DBT units and yellow from PTZ-DBTO2. As a result, the fluorescence of P3 varies from greenish-blue with 10% water, white with 60% water, to yellow with 90% water. This represents the first example of tuning the emission color of a TADF polymer by only adding water. Furthermore, the AEE phenomenon of P3 was also confirmed by PLQY data in the THF/water mixture with quinine sulphate as a reference standard. The PLQY value of P3 in the THF solution is low (2.4%) and increases with the content of water to 41.8% when the content of water is 90%. This result is consistent with the PL spectra. The CIE coordinates are shown in **Figure S6** and **Table S2**. The emission color of P3 films can also be controlled by doping with different ratios of poly(methyl methacrylate) (PMMA). **Figure 3c** shows that the fluorescence of P3 varies from greenish yellow with 10% PMMA to cool-white with 90% PMMA. This shows that PMMA can disperse and reduce ACQ of DBT units. Comparable spectra for P1 and P2 are shown in **Figure S7**.

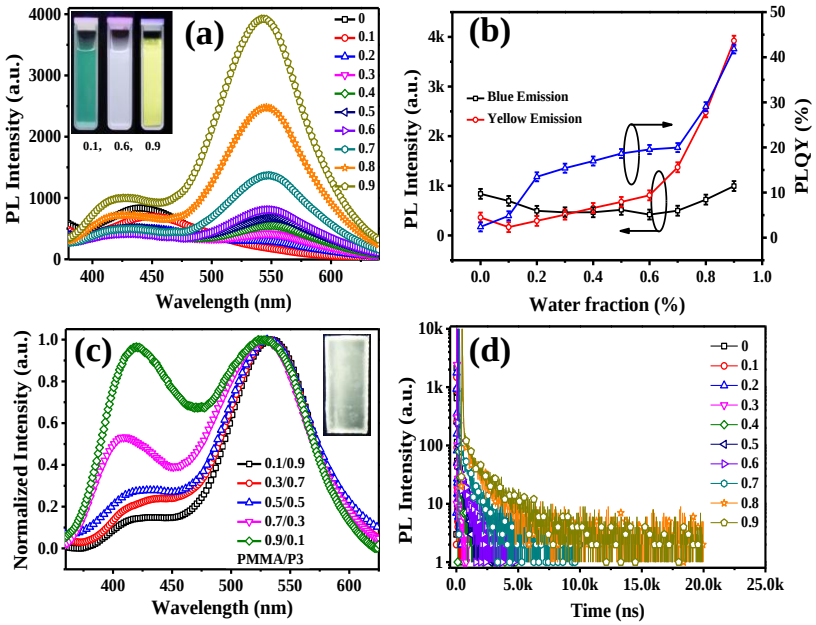

Figure 3. (a) PL spectra of P3 in THF/water mixtures with different fractions of water; the inset is fluorescent images of P3 in different THF/water mixtures under UV light irradiation. (b) Plots of PL intensity and PLQY versus the different water fractions for P3; (c) PL spectra of P3 in different contents of PMMA; inset is the PL image of 0.9PMMA/0.1P3 under UV light irradiation. (d) Transient photoluminescence decay curves at 550 nm for P3 with different THF/water ratios.

The transient PL decays of P3 in aqueous THF show that the excited state lifetimes are significantly enhanced with increasing water fraction (**Figure 3d**). In pure THF bi-exponential decays are observed for P3 with two distinct lifetimes of 9.25 ns and 35.61 ns. At ratios of 1:9 THF/water, the bi-exponential decay lifetimes increase to 32.56 ns and 1643 ns, respectively. When P3 aggregates, the non-radiative decay due to vibrations that affect the PTZ-DBTO2 units is effectively impeded, and thus the excitons are less quenched. Moreover, the lifetime of P3 in the aggregated state is longer than those of P1 and P2 (**Figure S8**). P3 has a larger contribution from TADF, consistent with reduced quenching of triplet states due to vibrations and triplet-triplet annihilation, a longer triplet lifetime leads to a longer DF lifetime and stronger emission.

2.5. Doped properties

For the fabrication of OLEDs using P1, P2 and P3, a TCTA/TAPC mixture was used as the host. The film-forming ability, morphological stability of solution-processed films of the copolymers doped with TCTA/TAPC (65/25wt%) were investigated by atomic force microscopy (AFM). The films were spin-coated from 10 mg/ml toluene solution with 2000 rpm and then annealed for 30 min at 120 °C. As shown in **Figure 4**, the AFM images display smooth and homogeneous morphology with small root-mean square (RMS) roughness values of 0.383 nm for P1, 0.454 nm for P2 and 0.446 nm for P3. It is free of particle aggregation or phase separation, suggesting both good film-forming ability and good miscibility. Thus, the mixture of TCTA/TAPC (65/25wt%) appears to be a suitable host for OLEDs.

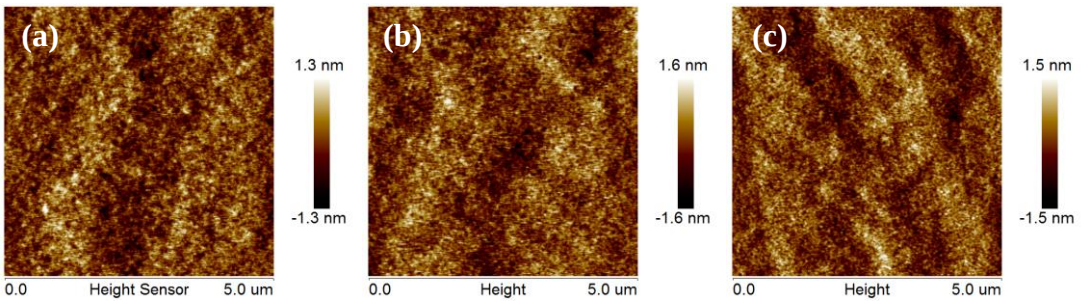

Figure 4. AFM height images of P1 (a), P2 (b) and P3 (c) doped with 65 wt% TATC and 35 wt% TAPC.

Figure 5a shows the time-dependent fluorescence decays of the copolymer thin films doped with TCTA/TAPC (65/25 wt%) at room temperature. The copolymers show longer TADF lifetimes in the hosts than as pure films (**Figure 2a**), probably due to effectively reduced triplet exciton annihilation through host dispersing. Furthermore, the contribution of delayed fluorescence (DF) to the overall emission of thin films of P1-P3/TCTA/TAPC (10/65/25 wt%) was evaluated. The DF contribution is 47% for P1, 54% for P2 and 56% for P3 (**Figure S9**). For the pure polymer films the DF contribution is 7%, 13% and 32%, respectively (**Figure S10**). The DF contribution in the hosts is considerably higher than that of

the pure films, indicating the hosts can effectively reduce triplet quenching due to triplet-triplet annihilation.

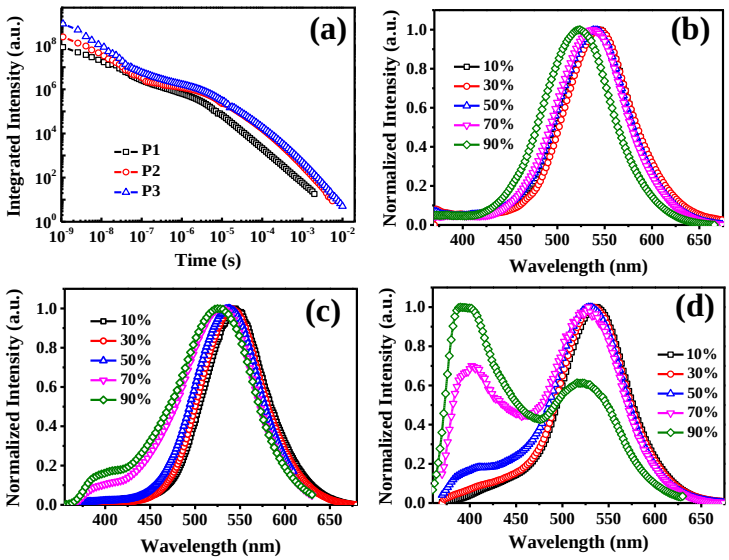

Figure 5. (a) Fluorescence decay data for copolymers/TCTA/TAPC (10/65/25wt%). PL spectra of P1 (b), P2 (c) and P3 (d) doped with the different ratio of host (65 wt% TATC and 35 wt% TAPC).

PL spectra of P1, P2 and P3 doped with a different ratio of mixture of TCTA/TAPC can be seen in **Figures 5b, c, d**. The emission color of P1 and P2 films show greenish yellow light with the increase of host, which is mainly derived from the strong emission of TADF units. This is consistent with their PMMA doped spectra. In contrast, fluorescence of P3 varies from greenish yellow to two-color white with adding the host, which confirms the stronger blue emission with increasing contents attribute to DBT units. The higher ratios of TCTA/TAPC efficiently disperse the DBT units and thus DBT emits strong blue light which is consistent with the result shown in **Figure 3c**.

2.6. OLED performances

As shown in **Figure 6a**, the OLED architecture is: ITO/PEDOT:PSS (40 nm)/polymer: TCTA: TAPC (10:65:25 wt%) (45 nm)/TmPyPB (50 nm)/LiF (0.8 nm)/Al (80 nm). A mixture of hole-transporting hosts tris(4-carbazol-9-yl-phenyl)amine (TCTA) and 4,4'-

cyclohexylidenebis[N,N-bis(4-methylphenyl) benzenamine] (TAPC) with high triplet energies of 2.78 and 2.87 eV were used to reduce the driving voltage and improve charge balance and injection.[27,48] PEDOT:PSS (poly(3,4-ethylenedioxythiophene:poly(styrene sulfonate)) and 1,3,5-tris(3-pyridyl-3-phenyl)benzene (TmPyPB) serve as the hole-injection layer and the electron-transport layer, respectively. TmPyPB also acts as an exciton blocking layer to prevent excitons quenching at the metal electrode interface.

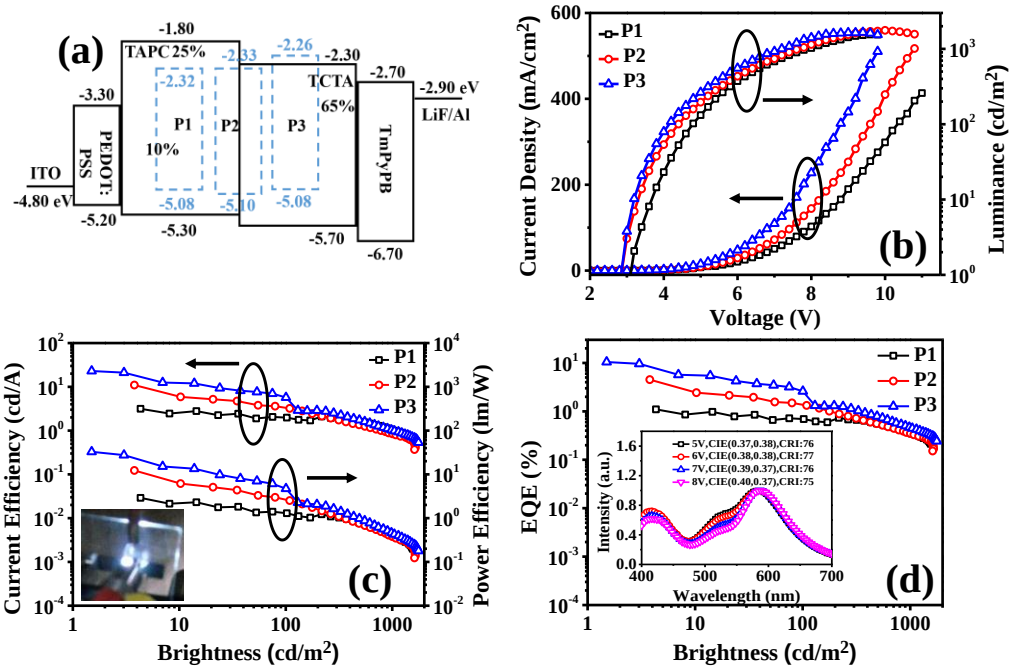

Figure 6. (a) Energy level diagram and structure of OLED devices. (b) Current density-voltage-luminance (*J-V-L*) curves. (c) Current and power efficiency versus brightness, the inset is the electroluminescence of P3; (d) External quantum efficiency (EQE) versus brightness; the inset is electroluminescent spectra of P3 at different voltages.

Current density versus voltage, and brightness versus voltage curves are shown in **Figure 6b**. All of the devices reach a maximum luminance of 1500 cd/m^2 and exhibit low turn-on voltages of 2.9-3.0 V. This may be attributed to the suitable HOMO level (-5.3 eV) which reduces the hole injection barrier from PEDOT:PSS (φ = -5.2 eV). **Figures 6c&d** depict the current and power efficiencies and the external quantum efficiencies with respect to brightness. The key EL parameters are summarized in **Table 2**. The best EL performance is

achieved for the P3 device with CE_{max} of 23.0 cd/A, PE_{max} of 32.8 lm/W, and EQE_{max} of 10.4%, and can be attributed to the high DF contribution and long TADF lifetime in the host. Furthermore, the EQE at the practically relevant brightness of 100 and 500 cd/m^2 are 2.6% and 0.8%, respectively.

P1 and P2 based OLEDs show yellow light with $CIE_{x,y}$ (0.46, 0.43) and (0.45, 0.40) (**Figure S11**) and P3 devices show warm-white light emission. Additionally, good color stability in the EL spectra of P3 devices is observed with the CIE coordinates varying from (0.37, 0.38) at 5 V to (0.40, 0.37) at 8 V (**Figure 6d**). Impressively, the WOLED has a high color rendering index (CRI) of 77 at 6 V, which is comparable with those of the reported two-color TADF WOLEDs (38 ~ 77).[23,49]

Compared with the corresponding PL spectra of P3/TCTA/TAPC and P3/PMMA films, the EL spectra of P3 exhibit a broad emission mainly located at 416 nm from DBT units, 535 nm from TADF units and a new peak at 580 nm. The emerging 580 nm emission could be caused by exciplex excitons formed between P3 and TmPyPB. However, the PL spectrum of P3/TmPyPB (1:1) **(Figure S12)** shows no 580 nm emission, which indicates that an exciplex is not formed between these two materials, nor between P3 and TCTA or TAPC.[50] Therefore, we tentatively assign the 580 nm peak in EL to the effect of the electric field on the randomly oriented dipole moments of the TADF units,[51] i.e. electroplex emission, or most probably due to the formation of an electromer, which cannot be observed in PL spectra. The formation of an electromeric state is observed usually when trapped carriers recombine under the interaction with an electric field, and cause the emission to red-shift with respect to photoluminescence[52, 53] Therefore, the white emission of the device originates from the combination of the CT and electromer emission. However, further studies are need to fully understand this effect in our materials.[54] According to the literature, when the HOMO (P3) – HOMO (TmPyPB) gap is smaller than LUMO (P3) – LUMO (TmPyPB) gap, the LUMO(EML) → LUMO(ETL) electron transfer rate is reduced to some extent enabling a

spatially cross electron transfer from the LUMO of EML to the HOMO of ETL, producing electroplex emission.[54] As shown in **Figure 6a**, the HOMO-LUMO alignment of P3 fits this rule well. In addition, the ratio of intensity of blue-green emissions and orange-red emissions in the EL spectra increases along with the voltage increasing, which is consistent with the nature of electric-field dependence of electroplex emission.[55, 56] Moreover, the EL spectrum of non-doped devices (ITO/PEDOT:PSS/P3/TmPyPB/LiF/Al) **(Figure S13)** show 580 nm emission as well, which again confirms the electroplex formation between P3 and TmPyPB. Therefore, electroplex formation has the benefit of making P3 to be warm-white (CIE_{xy}: 0.37, 0.38) instead of cool-white (CIE_{xy}: 0.25, 0.33) of PL. From previous publications, warm-white EL is desirable for comfortable ambient lighting that does not cause eye fatigue,[57, 58] while cool-white with too much blue can cause retinal damage.[59] Our work reports the first example of warm-white TADF polymer OLEDs.

Table 2. Device Performance Data.

	V_{on}[a] (V)	L_{max}[b] (cd/m^2)	CE_{max}[c] (cd/A)	PE_{max}[d] (lm/W)	EQE_{max}[e]	EQE_{100}[f]	EQE_{500}[f]	CIE[g] (x,y)
P1	3.1	1552	3.1	2.3	1.1	0.7	0.6	(0.46, 0.43)
P2	2.9	1764	11.0	12.3	4.5	1.3	0.6	(0.45, 0.40)
P3	2.9	1653	23.0	32.8	10.4	2.6	0.8	(0.37, 0.38)

[a]The voltage at 1 cd/m^2. [b]Maximum luminance. [c]Maximum current efficiency. [d]Maximum power efficiency. [e]Maximum external quantum efficiency. [f]External quantum efficiency at 100 and 500 cd/m^2. [g]CIE coordinates at 5 V.

3. Conclusion

In conclusion, we have synthesized a series of copolymers in which 2-(10H-phenothiazin-10-yl)dibenzothiophene-S,S-dioxide units give yellow TADF and AIE, while dibenzothiophene units act as a blue fluorophore and host. The emission of P3 in THF solution can be tuned by simply increasing the water fraction, varying from sky-blue through white to yellowish-green. The copolymerization of lower band-gap TADF monomers with higher band-gap fluorophor is a promising method to tune the light wavelength and realize white light-emitting from a single polymer. OLEDs based on P1 and P2 show yellow emission, while P3 OLEDs show two-color warm-white emission with high CRI of 77, CE_{max} of 23.0 cd/A, PE_{max} of 32.8

lm/W, EQE_{max} of 10.4% with CIE coordinates of (0.37, 0.38) at 5 V. Moreover, EQE of 2.6%, CE of 5.7 cd/A, PE of 4.7 lm/W at 100 cd/m^2 are obtained. Meanwhile, these new TADF copolymers provide guidelines to prepare higher efficiency polymeric TADF-based OLEDs and white emitters for displays and lighting. The macromolecular design is versatile allowing for a systematic variation of the steric and electronic properties of the spacer units, and their ratio in the copolymer structure: this could also be an effective strategy to tune the emission color.

4. Experimental Section

General synthetic procedure for the copolymers: A mixture of AIBN (10 mg, 0.06 mmol), toluene (8.0 mL) / THF (20 mL), and different ratios of 2-vinyldibenzothiophene (M1) and 2-(10*H*-phenothiazin-10-yl)-8-vinyldibenzothiophene-*S*,*S*-dioxide (M2) were placed in an ampule, which was cooled, degassed, and sealed *in vacuo*. After stirring at 60 °C for 20 h, the reaction mixture was poured into a large excess of methanol. The yellow polymer was obtained by filtration and then was dried *in vacuo*. The polymer was fractionated by Soxhlet extraction using hexane.

P1: M1 (660 mg, 1.5 mmol) and M2 (315 mg, 1.5 mmol) were used in the polymerization (yield: 81%). Elemental analysis. Found: C 69.47; H 6.43, N 2.39, S 13.58%.

P2: M1 (330 mg, 0.75 mmol) and M2 (630 mg, 3.0 mmol) were used in the polymerization (yield: 87%). Elemental analysis. Found: C 74.38; H 8.48, N 1.74, S 12.63%.

P3: M1 (198 mg, 0.45 mmol) and M2 (840 mg, 4.0 mmol) were used in the polymerization (yield: 83%). Elemental analysis. Found: C 76.69; H 5.94, N 0.93, S 13.93%.

Supporting Information

Supporting Information is available from the Wiley Online Library or from the author.

Acknowledgements

The financial support of the National Natural Science Foundations of China under Grant No. 51521062 is gratefully acknowledged. Work in Durham was funded by EPSRC grant EP/L02621X/1.

Received: ((will be filled in by the editorial staff))
Revised: ((will be filled in by the editorial staff))
Published online: ((will be filled in by the editorial staff))

References

[1] J. Kido, M. Kimura, K. Nagai, *Science* **1995**, *267*, 1332.

[2] Y. Sun, N. C. Giebink, H. Kanno, B. Ma, M. E. Thompson, S. R. Forrest, *Nature* **2006**, *440*, 908.

[3] S. Reineke, F. Lindner, G. Schwartz, N. Seidler, K. Walzer, B. Lüssem, K. Leo, *Nature* **2009**, *459*, 234.

[4] S. Y. Lee, T. Yasuda, Y. S. Yang, Q. Zhang, C. Adachi, *Angew. Chem., Int. Ed.* **2014**, *126*, 6520.

[5] K. V. Rao, K. Datta, M. Eswaramoorthy, S. J. George, *Adv. Mater.* **2013**, *25*, 1713.

[6] Q. Y. Yang, J. M. Lehn, *Angew. Chem., Int. Ed.* **2014**, *53*, 4572.

[7] M. Han, Y. Tian, Z. Yuan, L. Zhu, B. Ma, *Angew. Chem., Int. Ed.* **2014**, *53*, 10908.

[8] S. Shao, J. Ding, L. Wang, X. Jing, F. Wang, *J. Am. Chem. Soc.* **2012**, *134*, 20290.

[9] D. A. Poulsen, B. J. Kim, B. Ma, C. S. Zonte, J. M. J. Fréchet, *Adv. Mater.* **2010**, *22*, 77.

[10] L. Ying, C. L. Ho, H. Wu, Y. Cao, W. W. Wong, *Adv. Mater*. **2014**, *26*, 2459.

[11] R. Friend, R. Gymer, A. Holmes, J. Burroughes, R. Marks, C. Taliani, D. Bradley, D. Dos Santos, J. Bredas, M. Lögdlund, *Nature* **1999**, *397*, 121.

[12] M. A. Baldo, D. O'Brien, Y. You, A. Shoustikov, S. Sibley, M. Thompson, S. Forrest, *Nature* **1998**, *395*, 151.

[13] S. Schmidbauer, A. Hohenleutner, B. König, *Adv. Mater.* **2013**, *25*, 2114.

[14] H. Uoyama, K. Goushi, K. Shizu, H. Nomura, C. Adachi, *Nature* **2012**, *492*, 234.

[15] Q. Zhang, B. Li, S. Huang, H. Nomura, H. Tanaka, C. Adachi, *Nature Photon.* **2014**, *8*, 326.

[16] F. B. Dias, K. N. Bourdakos, V. Jankus, K. C. Moss, K. T. Kamtekar, V. Bhalla, J. Santos, M. R. Bryce, A. P. Monkman, *Adv. Mater.* **2013**, *25*, 3707.

[17] F. B. Dias, J. Santos, D. R. Graves, P. Data, R. S. Nobuyasu, M. A. Fox, A. S. Batsanov, T. Palmeira, M. N. Berberan-Santos, M. R, Bryce, A. P. Monkman, *Adv. Sci.* **2016**, *3*, 1600080.

[18] J. Nishide, H. Nakanotani, Y. Hiraga and C. Adachi, *Appl. Phys. Lett.*, 2014, **104**, 233304.

[19] Y. J. Cho, K. S. Yook, J. Y. Lee, *Sci. Rep.* **2015**, *5*, 7859.

[20] B. S. Kim, K. S. Yook, J. Y. Lee, *Sci. Rep.* **2014**, *4*, 6019.

[21] D. Zhang, L. Duan, Y. Li, D. Zhang, Y. Qiu, *J. Mater. Chem. C* **2014**, *2*, 8191.

[22] X. L. Li, G. Xie, M. Liu, D. Chen, X. Cai, J. Peng, Y. Cao, S. J. Su, *Adv. Mater.* **2016**, *28*, 4614.

[23] X. K. Liu, W. Chen, H. T. Chandran, J. Qing, Z. Chen, X. H. Zhang, C. S. Lee, *ACS Appl. Mater. Interfaces* **2016**, *8*, 26135.

[24] C. Grimsdale, K. Leok Chan, R. E. Martin, P. G. Jokisz and A. B. Holmes, *Chem. Rev.* **2009**, *109*, 897.

[25] G. Xie, J. Luo, M. Huang, T. Chen, K. Wu, S. Gong, C. Yang, *Adv. Mater.* **2017**, DOI: 10.1002/adma.201604223

[26] E. Nikolaenko, M. Cass, F. Bourcet, D. Mohamad, M. Roberts, *Adv. Mater.* **2015**, *27*, 7236.

[27] S. Y. Lee, T. Yasuda, H. Komiyama, J. Lee, C. Adachi, *Adv. Mater.* **2016**, *28*, 4019.

[28] J. Luo, G. Xie, S. Gong, T. Chen, C. Yang, *Chem. Commun.* **2016**, *52*, 2292.

[29] Y. Zhu, Y. Zhang, B. Yao, Y. Wang, Z. Zhang, H. Zhan, B. Zhang, Z. Xie, Y. Wang, Y. Cheng, *Macromolecules* **2016**, *49*, 4373.

[30] Z. Ren, R. S. Nobuyasu, F. B. Dias, A. P. Monkman, S. Yan, M. R. Bryce, *Macromolecules* **2016**, *49*, 5452.

[31] Z. Xie, C. Chen, S. Xu, J. Li, Y. Zhang, S. Liu, J. Xu, Z. Chi, *Angew. Chem., Int. Ed.* **2015**, *54*, 7181.

[32] S. Xu, T. Liu, Y. Mu, Y. F. Wang, Z. Chi, C. C. Lo, S. Liu, Y. Zhang, A. Lien and J. Xu, *Angew. Chem., Int. Ed.* **2015**, *54*, 874.

[33] R. Furue, T. Nishimoto, I. S. Park, J. Lee, T. Yasuda, *Angew. Chem., Int. Ed.* **2016**, *55*, 7171.

[34] S. Gan, W. Luo, B. He, L. Chen, H. Nie, R. Hu, A. Qin, Z. Zhao and B. Z. Tang, *J. Mater. Chem. C* **2016**, *4*, 3705.

[35] Y. Hong, J. W. Lam and B. Z. Tang, *Chem. Soc. Rev.* **2011**, *40*, 5361.

[36] Y. Hong, J. W. Lam and B. Z. Tang, *Chem. Commun.* **2009**, 4332.

[37] J. Mei, Y. Hong, J. W. Lam, A. Qin, Y. Tang, B. Z. Tang, *Adv. Mater.* **2014**, *26*, 5429.

[38] R. S. Nobuyasu, Z. Ren, G. C. Griffiths, A. S. Batsanov, P. Data, S. Yan, A. P. Monkman, M. R. Bryce, F. B. Dias, *Adv. Opt. Mater.* **2016**, *4*, 597.

[39] J. S. Ward, R. S. Nobuyasu, A. S. Batsanov, P. Data, A. P. Monkman, F. B. Dias, M. R. Bryce, *Chem. Commun.* **2016**, *52*, 2612.

[40] H. Tong, Y. Hong, Y. Dong, Y. Ren, M. Häussler, J. W. Lam, K. S. Wong, B. Z. Tang, *J. Phys. Chem. B* **2007**, *111*, 2000.

[41] S. Li, Y. Shang, E. Zhao, R. T. Kwok, J. W. Lam, Y. Song, B. Z. Tang, *J. Mater. Chem. C* **2015**, *3*, 3445.

[42] K. S. Yook, J. Y. Lee, *Adv. Mater.* **2012**, *24*, 3169.

[43] W. Yang, Q. Hou, C. Liu, Y. Niu, J. Huang, R. Yang, Y. Cao, *J. Mater. Chem.* **2003**, *13*, 1351.

[44] L. Wang, Z. Y. Wu, W. Y. Wong, K. W. Cheah, H. Huang, C. H. Chen, *Org. Electron.* **2011**, *12*, 595.

[45] S. H. Jeong, J. Y. Lee, *J. Mater. Chem.* **2011**, *21*, 14604.

[46] C. Han, Z. Zhang, H. Xu, S. Yue, J. Li, P. Yan, Z. Deng, Y. Zhao, P. Yan, S. Liu, *J. Am. Chem. Soc.* **2012**, *134*, 19179.

[47] F. B. Dias, *Phil. Trans. R. Soc. A* **2015**, *373*, 20140447.

[48] Q. Fu, J. Chen, C. Shi, D. Ma, *ACS Appl. Mater. Interfaces* **2012,** *4*, 6579.

[49] T. Peng, Y. Yang, H. Bi, Y. Liu, Z. Hou, Y. Wang, *J. Mater. Chem.* **2011**, *21*, 3551.

[50] N. Matsumoto, M. Nishiyama, C. Adachi, *J. Phys. Chem. C* **2008,** *112*, 7735.

[51] H. A. Al Attar, A. P. Monkman, *Adv. Mater.* **2016**, *28*, 8014.

[52] E. Angioni, M. Chapran, K. Ivaniuk, N. Kostiv, V. Cherpak, P. Stakhira, A. Lazauskas, S. Tamulevičius, D. Volyniuk, N. J. Findlay, T. Tuttle, J. V. Grazulevicius and P. J. Skabara, *J. Mater. Chem. C* **2016**, *4*, 3851.

[53] D. M. Shin, *J. Nanosci. Nanotechnol.* 2010, *10*, 6794.

[54] C.-C. Yang, C.-J. Hsu, P.-T. Chou, H. C. Cheng, Y. O. Su, M.-k. Leung, *J. Phys. Chem. B* **2010,** *114*, 756.

[55] J. Kalinowski, M. Cocchi, P. Di Marco, W. Stampor, G. Giro, V. Fattori, *J. Phys. D: Appl. Phys.* **2000**, *33*, 2379.

[56] S. Yang, X. Zhang, Y. Hou, Z. Deng, X. Xu, *J. Appl. Phys.* **2007,** *101*, 096101.

[57] L. S. Cui, Y. Liu, X. Y. Liu, Z. Q. Jiang, L. S. Liao, *ACS Appl. Mater. Interfaces* **2015**, *7*, 11007.

[58] X. K. Liu, Z. Chen, J. Qing, W. J. Zhang, B. Wu, H. L. Tam, F. Zhu, X. H. Zhang, C. S. Lee, *Adv. Mater.* **2015**, *27*, 707.

[59] I. Jaadane, P. Boulenguez, S. Chahory, S. Carre, M. Savoldelli, L. Jonet, F. Behar-Cohen, C. Martinsons, A. Torriglia, *Free Radic. Biol. Med.* **2015**, *84*, 373.

The first TADF polymer giving white emission and aggregation enhanced emission is reported. Solution-processable single-polymer warm-white organic light-emitting diodes (WOLEDs) exhibit a low turn-on voltage of 2.9 V and high CRI of 77 with CIE coordinates of (0.37, 0.36). This work provides a guide to prepare high efficiency polymeric TADF-based WOLEDs.

Chensen Li, Roberto S. Nobuyasu, Yukun Wang, Fernando B. Dias, Zhongjie Ren,* Martin R. Bryce,* Shouke Yan *

Solution-Processable Thermally Activated Delayed Fluorescence White OLEDs Based on Dual-Emission Polymers with Tunable Emission Colors and Aggregation Enhanced Emission Properties

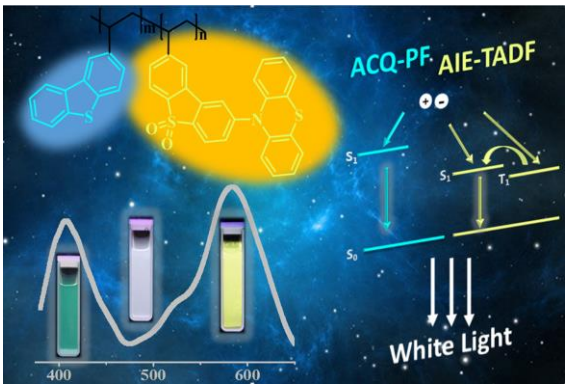

Supporting Information

Solution-Processable Thermally Activated Delayed Fluorescence White OLEDs Based on Dual-Emission Polymers with Tunable Emission Colors and Aggregation Enhanced Emission Properties

Chensen Li, Roberto S. Nobuyasu, Yukun Wang, Fernando B. Dias, Zhongjie Ren, Martin R. Bryce,* Shouke Yan **

Materials

All reactants (Adamas-beta) were purchased from Adamas Reagent, Ltd without further purification and all solvents were supplied by Beijing Chemical Reagent Co., Ltd. Anhydrous and deoxygenated solvents were obtained by distillation over a sodium benzophenone complex.

Characterization

^{1}H NMR spectra were recorded on a Bruker AV400 (400 MHz) spectrometer. Chemical shifts (δ) are given in parts per million (ppm) relative to tetramethylsilane (TMS; δ = 0) as the internal reference. ^{1}H NMR spectral data are reported as chemical shift, relative integral, multiplicity (s = singlet, d = doublet, m = multiplet), coupling constant (*J* in Hz) and assignment. Elemental analyses of carbon, hydrogen, nitrogen and sulfur were performed on a Vario EL cube. UV/Vis absorption spectra were recorded on a Hitachi U-2910 spectrophotometer. PL spectra were recorded on a Hitachi F-7000 fluorescence spectrophotometer. The temperature dependence of transient PL decay curves in different THF/water mixture and PL spectra in vacuum/air was determined using a spectrometer (FLS980) from Edinburgh Instruments Limited. The fluorescence quantum yields of solid films were measured on FLS980 with an integrating sphere (φ = 150 mm). Phosphorescence,

prompt fluorescence (PF), and delayed fluorescence (DF) spectra and decays were recorded using nanosecond gated luminescence and lifetime measurements (from 400 ps to 1 s) with either a high-energy pulsed Nd:YAG laser emitting at 355 nm (EKSPLA) or a N2 laser emitting at 337 nm. Emission was focused onto a spectrograph and detected on a sensitive gated iCCD camera (Stanford Computer Optics) having subnanosecond resolution. PF/DF time-resolved measurements were performed by exponentially increasing the gate and delay times. The CIE coordinates were obtained using CIE1931xy.V.1.6.0.2 application program. Differential scanning calorimetry (DSC) was performed on a TA Q2000 differential scanning calorimeter at a heating rate of 10 °C min^{-1} from 25 to 310 °C under nitrogen atmosphere. The glass transition temperature (T_g) was determined from the second heating scan. Thermogravimetric analysis (TGA) was undertaken with a METTLER TOLEDO TGA/DSC 1/1100SF instrument. The thermal stability of the samples under a nitrogen atmosphere was determined by measuring their weight loss while heating at a rate of 10 °C min^{-1} from 25 to 800 °C. Cyclic voltammetry (CV) was carried out in nitrogen-purged acetonitrile at room temperature with a CHI voltammetric analyser. Tetrabutylammonium hexafluorophosphate ($TBAPF_6$ 0.1 M) was used as the supporting electrolyte. The conventional three-electrode configuration consists of a glassy carbon working electrode, a platinum wire auxiliary electrode, and an $Ag/AgNO_3$ pseudo-reference electrode. Cyclic voltammograms were obtained at scan rate of 100 mV s^{-1}. The onset potential was determined from the intersection of two tangents drawn at the rising and background current of the cyclic voltammogram. The oxidation and reduction behaviors of polymers were firstly determined in the $TBAPF_6$ acetonitrile solution and then ferrocene was added into the same solution to confirm the potential. Gel permeation chromatography (GPC) analysis was carried out on a Waters 515-2410 system using polystyrene standards as molecular weight references and tetrahydrofuran (THF) as the eluent.

Device Fabrication and Characterization

The hole-injection material PEDOT:PSS (Al 4083) and electron-transporting and hole-blocking material TmPyPB were obtained from commercial sources. ITO-coated glass with a sheet resistance of 10 Ω per square was used as the substrate. Before device fabrication, the ITO-coated glass substrate was precleaned and exposed to UV-ozone for 2 min. PEDOT:PSS was then spin-coated onto the clean ITO substrate as a hole-injection layer. Next, a mixture of 10% polymer, 25% TAPC and 65% TCTA in toluene was spin-coated (10 mg/mL; 1500 rpm) to form a ca. 45 nm thick emissive layer and annealed at 80 °C for 30 min to remove the residual solvent. Finally, a 30 nm thick electron-transporting layer of TmPyPB was vacuum deposited, and a cathode composed of a 1 nm thick layer of LiF and aluminum (100 nm) was sequentially deposited through shadow masking with a pressure of 10^{-6} Torr. The current density-voltage-luminance (*J-V-L*) characteristics of the devices were measured using a Keithley 2400 Source meter and a Keithley 2000 Source multimeter. The EL spectra were recorded using a JYSPEX CCD3000 spectrometer. The EQE values were calculated from the luminance, current density, and electroluminescence spectrum according to previously reported methods.[1] All measurements were performed at room temperature under ambient conditions.

Supporting Figures

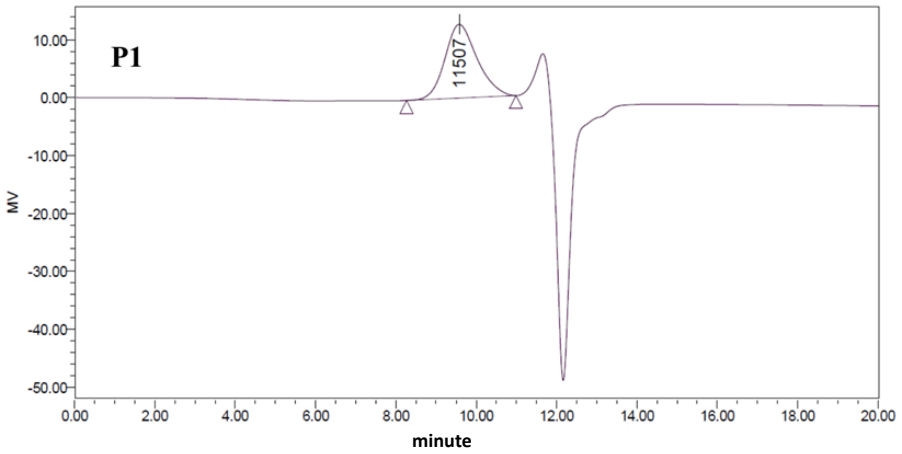

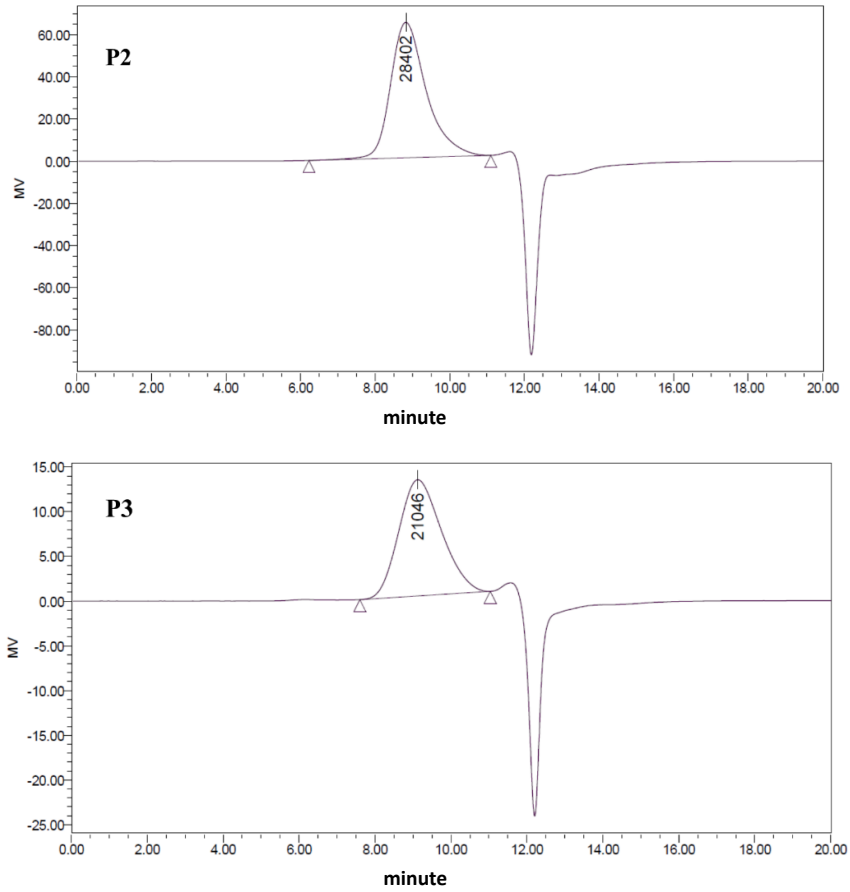

Figure S1. GPC chromatograms of P1, P2 and P3.

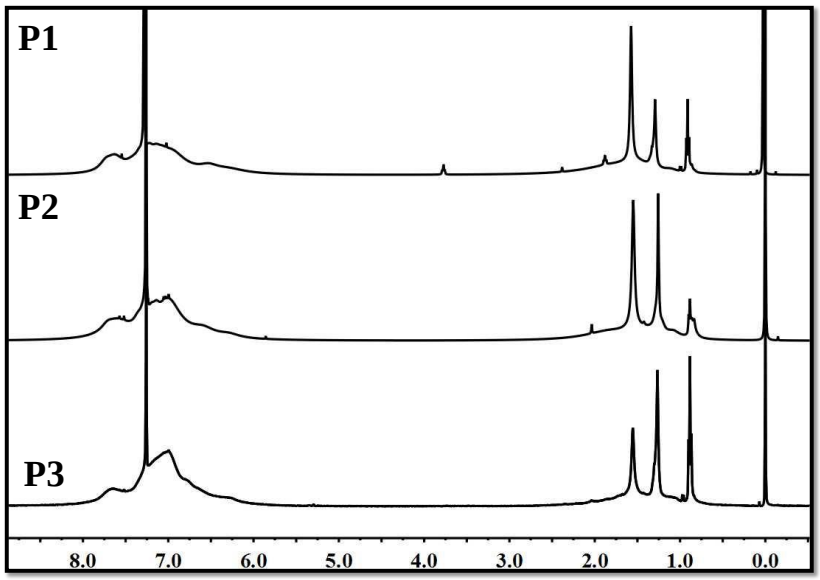

Figure S2. ^{1}H NMR spectra of P1, P2 and P3.

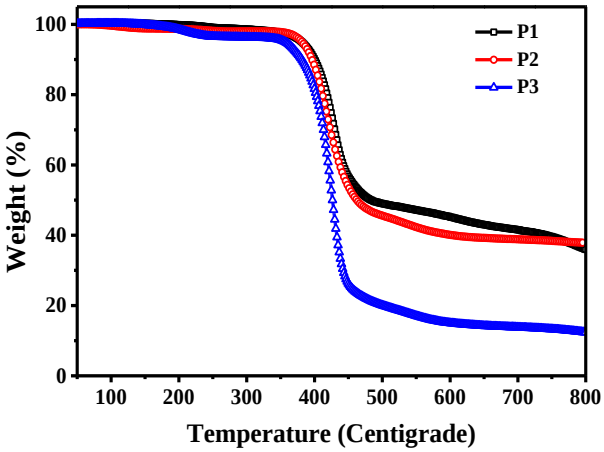

Figure S3. TGA traces of P1, P2 and P3 recorded at a heating rate of 10 °C min^{-1}.

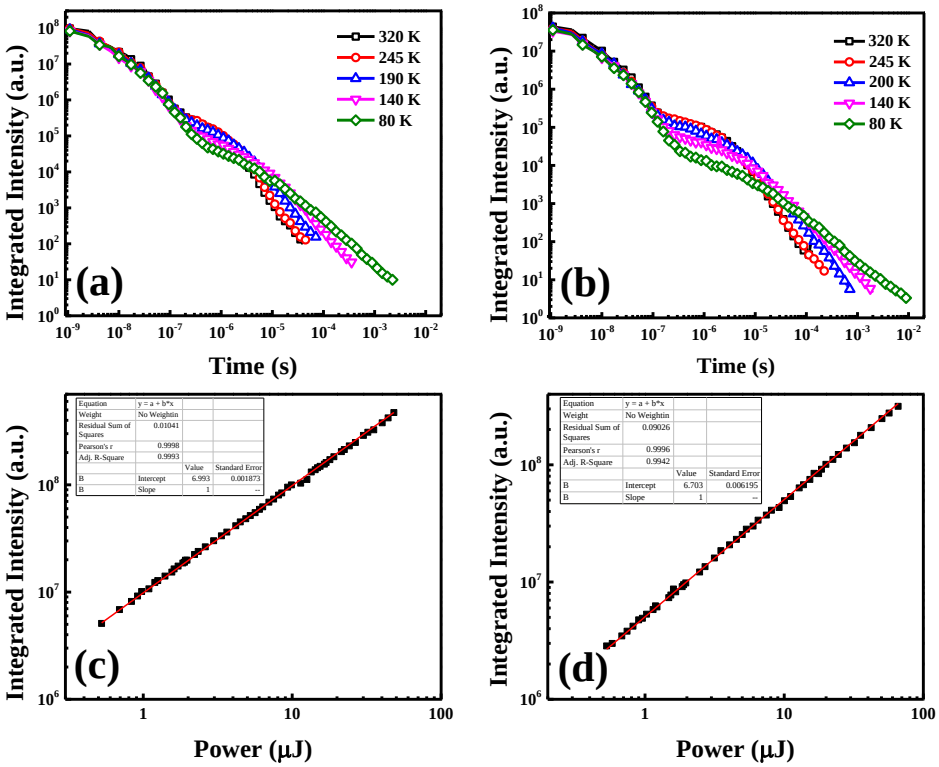

Figure S4. Temperature dependence of P1 (a) and P2 (b) fluorescence decays. Power dependence of DF for P1 (c) and P2 (d).

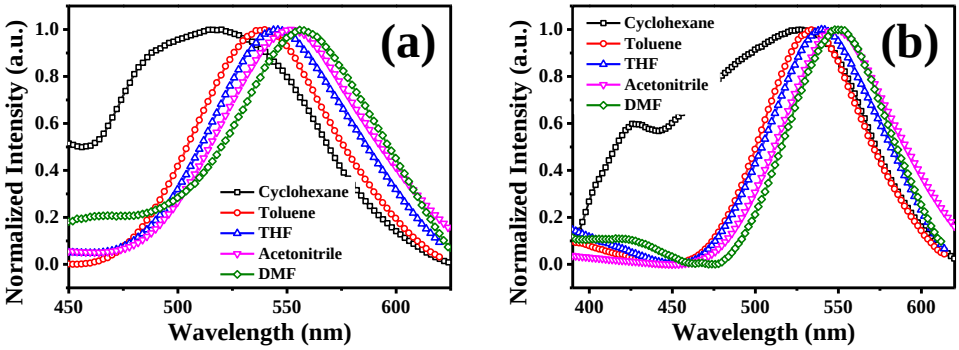

Figure S5. Photoluminescence spectra of P1 (a) and P2 (b) in cyclohexane, toluene, THF, acetonitrile and DMF with 0.1 mg/ml (excited at 325 nm).

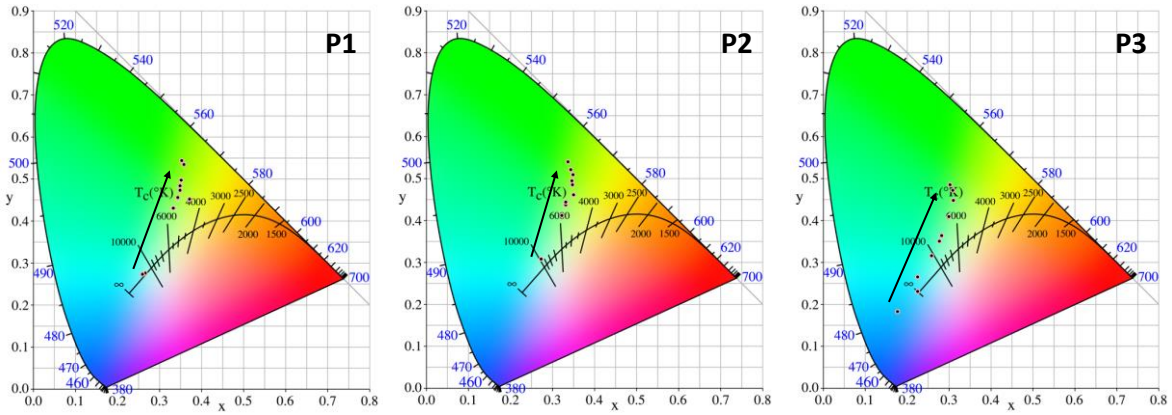

Figure S6. Calculated PL emission color coordinates of P1, P2 and P3 in THF/water mixtures in the CIE 1931 chromaticity diagram (direction of arrow indicate increasing water fraction).

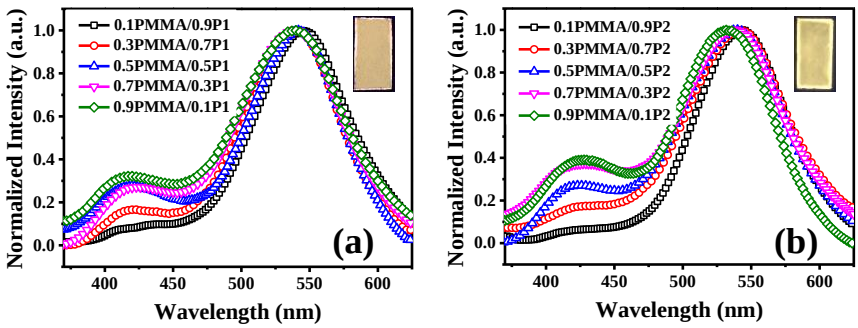

Figure S7. Photoluminescence spectra and fluorescence images of P1 (a), P2 (b) in different contents of PMMA (excited at 325 nm). Inset are the PL images of 0.9PMMA/0.1P1 and 0.9PMMA/0.1P2 under UV light irradiation.

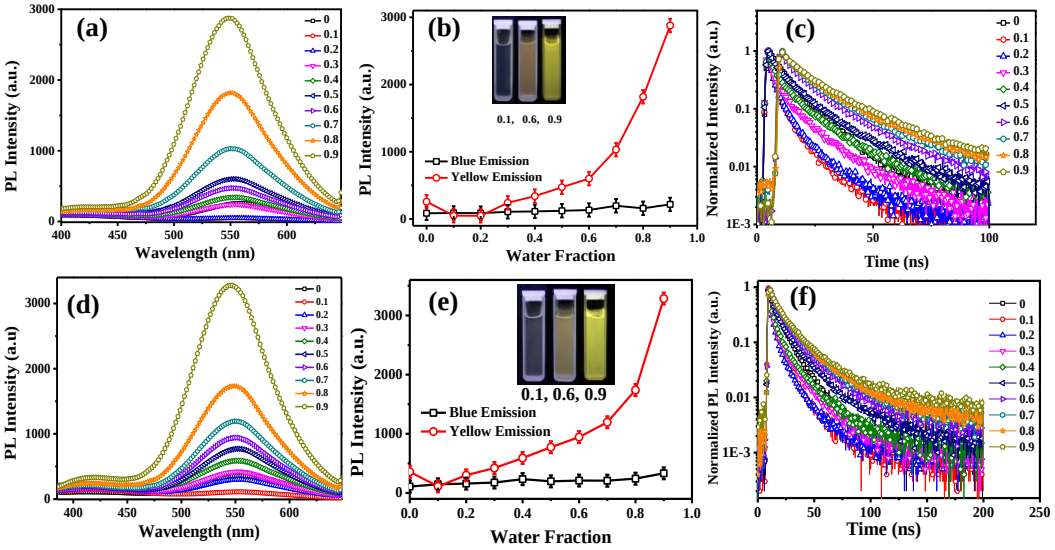

Figure S8. Photoluminescence spectra of P1 (a) and P2 (d) in THF/water mixtures with different amounts of water; plot of PL intensity versus the different water fractions of P1 (b)

and P2 (e), and fluorescence images of P1 and P2 in different THF/water mixture under UV light irradiation (inset). Transient photoluminescence decay (excited at 340 nm) curves at 550 nm for P1 (c) and P2 (f) in aqueous THF with different THF/water ratios.

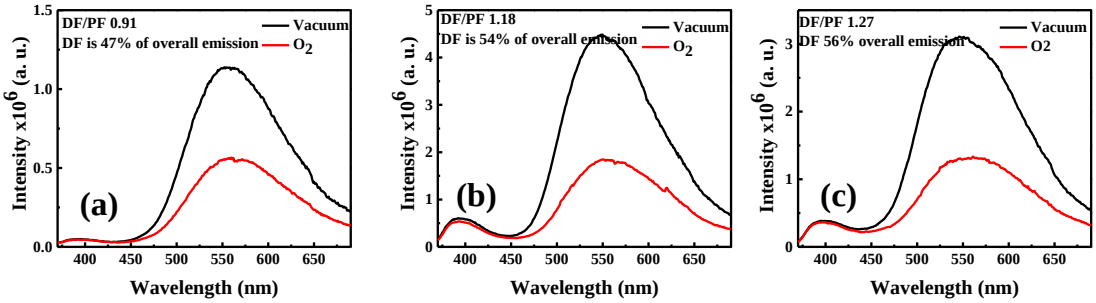

Figure S9. Spectra of integrated prompt and delayed fluorescence (PF and DF) of P1 (a), P2 (b) and P3 (c) doped at 10wt% with hosts (TCTA/TAPC: 65/25wt%) obtained from time-resolved fluorescence decays.

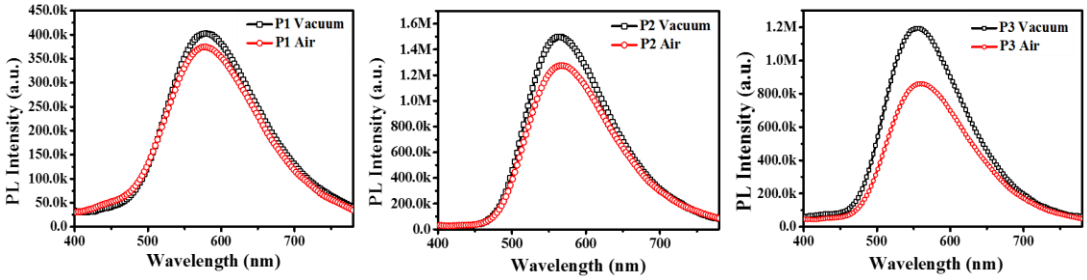

Figure S10. PL spectra of film of P1, P2 and P3 in air atmosphere and under vacuum. The calculated emission ratio of DF is 7% in P1, 13% in P2 and 32% in P3. The overall luminescence of the PTZ-DBTO2 units in the polymers has a strong contribution from the triplet state (TADF). Moreover, the calculated ratio of DF decreases with a reduction in the content of DBT units which may be assigned to the DBT units dispersing the TADF units and thus preventing triplet-triplet annihilation.

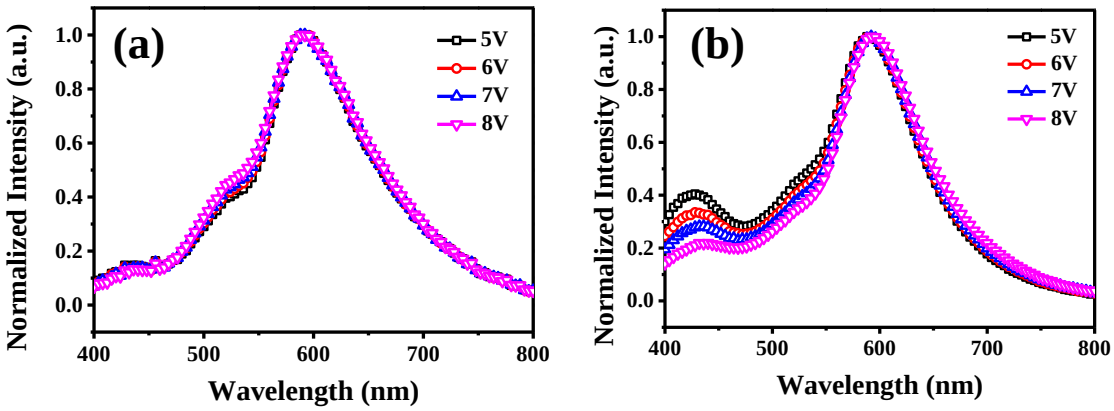

Figure S11. The electroluminescent spectra of P1 (a) and P2 (b) at different driving voltages.

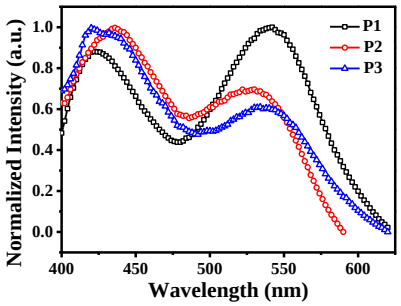

Figure S12. PL spectra of P1, P2 and P3 doped with host and TmPyPB.

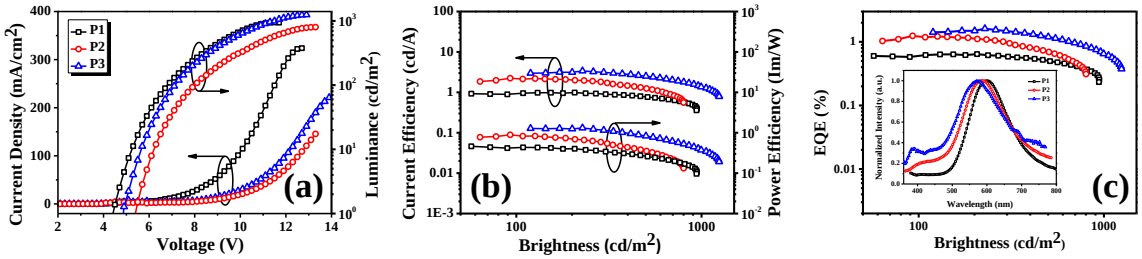

Figure S13. Non-doped devices data: (a) Current density-voltage-luminance (*J-V-L*) curves; (b) Current and power efficiency versus brightness; (c) External quantum efficiency (EQE) versus brightness; the inset is electroluminescent spectra of P1-3 at 6 V.

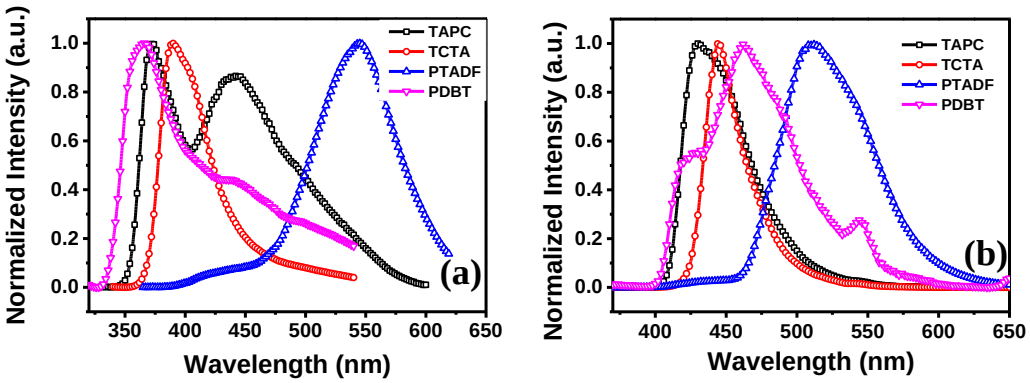

Figure S14. PL spectra (a) and phosphorescence spectra (b) of TAPC, TCTA, PTADF and PDBT. (PTADF is the homopolymer of 2-(10*H*-phenothiazin-10-yl)-8-vinyldibenzothiophene-*S*,*S*-dioxide (PTZ-DBTO2).[1] PDBT is the homopolymer of 2-vinyldibenzothiophene.

Synthetic Scheme and Procedures

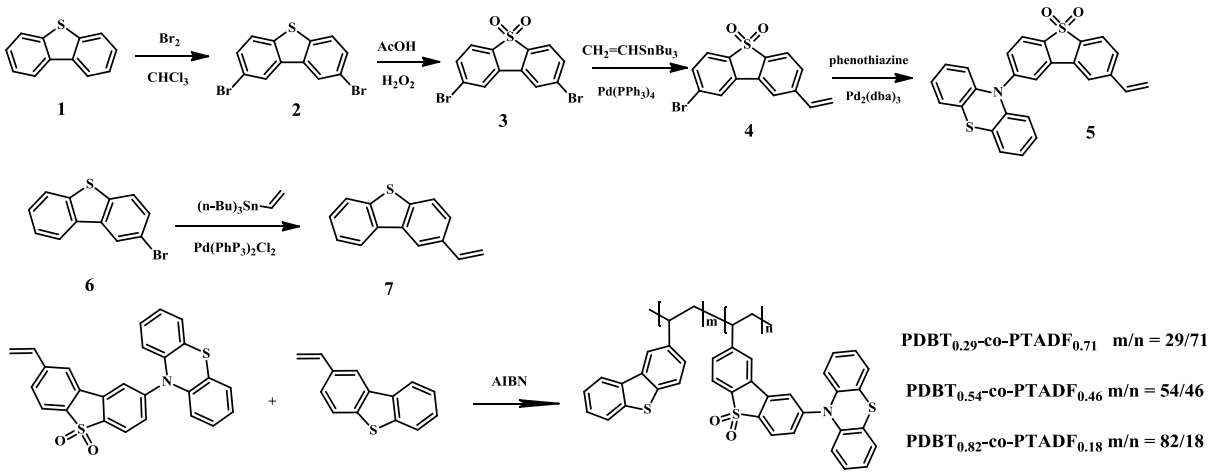

Scheme S1. Synthetic routes of monomers and copolymers.

2,8-Dibromo-dibenzothiophene (2) and 2,8-Dibromo-dibenzothiophene-*S*,*S*-dioxide (3) were prepared according to the reference.[2]

2-Bromo-8-vinyldibenzothiophene-*S*,*S*-dioxide (4) and 2-(10*H*-Phenothiazin-10-yl)-8-vinyldibenzothiophene-*S*,*S*-dioxide (5) were prepared following the procedures in reference[1].

2-Bromodibenzothiophene (6) was prepared according to the reference.[3]

2-Vinyldibenzothiophene (7):[3] In the absence of light, a solution of tri-*n*-butyl(vinyl)tin (1.05 mg, 3.3 mmol), 2-bromodibenzothiophene (868 mg, 3.3 mmol), 2,6-di-*tert*-butylphenol (6.8 mg, 0.033 mmol) and $[PdCl_2(PPh_3)_2]$ (93 mg, 0.14 mmol) in anhydrous toluene (50 mL) was stirred for 24 h at 100 °C. The mixture was cooled to room temperature and then poured into a large amount of water for extraction with DCM. The organic extracts were washed with aqueous KF solution and brine and then dried over $MgSO_4$. After evaporating the solvent, the residue was purified by column chromatography on silica gel with petroleum as eluent to afford the product (442 mg, 64%) as a white solid. ^{1}H NMR ($CDCl_3$, 400 MHz): δ 8.15 (m, 1H), 8.11 (d, 1H, *J* = 1.6 Hz), 7.84 (m, 1H), 7.78 (d, *J*=8.0 Hz, 1H), 7.55 (dd, *J* = 8.4, 1.6 Hz, 1H), 7.44 (m, 2H), 6.89 (dd, *J* = 10.8, 17.6 Hz, 1H), 5.87 (d, *J* =17.6 Hz, 1H), 5.32 (d, *J* = 11.2 Hz, 1H). ^{13}C NMR ($CDCl_3$, 100 MHz): δ 118.4, 121.5, 122.7, 124.3, 124.5, 124.6, 127.2, 129.5, 134.5, 137.2, 138.3, 139.9; m.p. 42.0-43.0 ^{o}C.

PTADF was prepared as reported previously.[4]

PDBT was prepared as reported previously.[3]

Table S1. Absolute PL quantum yield of P1, P2 and P3 in different solution determined by a calibrated integrating sphere in air.

	$\Phi_{PL,\ cyclohexane}$ (%)	$\Phi_{PL,\ toluene}$ (%)	$\Phi_{PL,\ THF}$ (%)	$\Phi_{PL,\ acetonitrile}$ (%)	$\Phi_{PL,\ DMF}$ (%)
P1	21.7	9.9	9.2	7.2	4.8
P2	33.9	16.1	17.4	7.7	6.0
P3	32.2	15.9	13.4	7.6	6.2

Table S2. Calculated PL emission color coordinates of P1, P2 and P3 in THF/water mixtures in the CIE 1931 chromaticity diagram. (0 = pure THF; 0.9 = THF/water 0.1/0.9).

Polymers	0	0.1	0.2	0.3	0.4	0.5	0.6	0.7	0.8	0.9
P1	(0.37,0.45)	(0.27,0.28)	(0.26,0.27)	(0.33,0.43)	(0.34,0.46)	(0.35,0.47)	(0.35,0.48)	(0.35,0.50)	(0.36,0.53)	(0.35,0.54)
P2	(0.35,0.46)	(0.27,0.31)	(0.32,0.41)	(0.33,0.44)	(0.33,0.44)	(0.35,0.49)	(0.35,0.50)	(0.35,0.51)	(0.34,0.52)	(0.34,0.54)
P3	(0.23,0.23)	(0.18,0.18)	(0.23,0.26)	(0.26,0.32)	(0.28,0.35)	(0.28,0.36)	(0.30,0.41)	(0.31,0.45)	(0.31,0.47)	(0.30,0.49)

Table S3. The transient photoluminescence decay times of P1, P2 and P3 in aqueous THF with different THF/water ratios (Unit: ns). (0 = pure THF; 0.9 = THF/water 0.1/0.9).

P1	**0**	**0.1**	**0.2**	**0.3**	**0.4**	**0.5**	**0.6**	**0.7**	**0.8**	**0.9**
τ_1	6.3	3.2	3.8	4.0	5.3	5.9	8.8	8.8	9.9	12.6
τ_2	14.2	11.1	12.8	14.4	16.4	17.5	22.2	22.6	25.5	31.7
P2	0	0.1	0.2	0.3	0.4	0.5	0.6	0.7	0.8	0.9
τ_1	6.9	4.4	4.8	5.0	5.1	7.6	9.1	10.0	9.7	9.7
τ_2	17.3	14.4	16.6	18.1	18.3	21.3	23.6	26.1	25.2	26.4
P3	0	0.1	0.2	0.3	0.4	0.5	0.6	0.7	0.8	0.9
τ_1	9.3	3.2	3.6	16.7	15.4	16.4	17.0	20.0	29.6	32.5
τ_2	35.6	11.2	16.3	275.3	327.8	434.4	483.3	769.2	1226	1643

Table S4. Non-doped Device Performance Data.

	V_{on}[a] (V)	L_{max}[b] (cd/m^2)	CE_{max}[c] (cd/A)	PE_{max}[d] (lm/W)	λ_{max} (nm)	EQE_{max}[e] (%)	CIE[f] (x,y)
P1	4.4	945	1.0	0.5	600	0.6	(0.48,0.45)
P2	5.4	801	2.2	0.9	585	1.2	(0.42,0.44)
P3	4.8	1246	3.4	1.3	570	1.6	(0.39,0.42)

[a]The voltage at 1 cd/m^2. [b]Maximum luminance. [c]Maximum current efficiency. [d]Maximum power efficiency. [e]Maximum external quantum efficiency. [f]CIE coordinates at 6 V.

References for Supporting Information:

[1] R. S. Nobuyasu, Z. Ren, A. S. Batsanov, P. Data, A. P. Monkman, M. R. Bryce, S. Yan

F. B. Dias, *Adv. Opt. Mater.* **2016**, *4*, 597-607.

[2] H. Liu, J. H. Zou, W. Yang, H. B. Wu, C. Li, B. Zhang, J. B. Peng, Y. Cao, *Chem. Mater.* **2008**, *20*, 4499-4506.

[3] O. Shimomura, T. Sato, I. Tomita, M. Suzuki, T. Endo, *J. Polym. Sci., Part A: Polym. Chem.* **1997**, *35*, 2813-2819.

[4] Z. Ren, R. S. Nobuyasu, F. B. Dias, A. P. Monkman, S. Yan, M. R. Bryce, *Macromolecules* **2016**, *49*, 5452-5460.